Design and Development of the INTELSAT V Graphite-Epoxy Central Thrust Tube

N. Barberis*
Ford Aerospace & Communications Corporation, Palo Alto, California
and
M. Zilani† and C. Gabriel‡
Société Nationale Industrielle Aerospatiale, Cannes, France

This paper describes the design, development, and testing of a graphite-epoxy central thrust tube for use on the INTELSAT VA spacecraft. The tube is the primary load path for the spacecraft and is a graphite-epoxy faceskin aluminum honeycomb structure designed to replace the aluminum cylinder/stringer stiffened tube at a net weight savings in excess of 9 kg. A prototype tube has been fabricated and successfully tested to ultimate static loads and a low level sine vibration test while integrated in the INTELSAT V Proto Engineering Model (PEM) spacecraft.

Introduction

THE complement of 15 spacecraft in the INTELSAT V series,[1] presently on order, will actually consist of three distinct types, whose capabilities have been gradually expanded. This growth has been made possible by increases of launch vehicle capabilities, as well as the orderly introduction of advanced technology and the inherent design margins in the initial body-stabilized spacecraft. The third "block" of spacecraft, designated INTELSAT VA,[2] incorporate an enhanced communications payload plus several product improvements, the most notable being replacement of the aluminum cylinder/stringer stiffened thrust tube with a graphite-epoxy honeycomb structure. The primary design requirements are a structurally optimized design yielding a 9 kg mass savings over the existing aluminum structure and full interchangeability with the present tube; thereby minimizing the impact of the graphite tube on the spacecraft design and integration.

INTELSAT V (Fig. 1) is a high-capacity commercial communications satellite. The 1800+ kg body-stabilized satellite, depending upon the operational configuration chosen by Intelsat, will carry up to 23,200 two-way telephone circuits using time division multiple access (TDMA) and two color television transmissions. The spacecraft communications subsystem operates at 6/4 GHz, expanding the available 500 MHz frequency band to 1.357 GHz through four-fold frequency reuse, involving spatial isolation (shaped beams) and polarization diversity (orthogonal circular). In addition, INTELSAT V uses 14/11 GHz "spot" beams with an additional 780 MHz of bandwidth plus a Maritime package with a shore-to-ship link operating at 6417.5-6425.0 MHz uplink and 1575.0-1542.5 MHz downlink; and a ship-to-shore link operating at 1636.5-1644.5 MHz uplink and 4192.5-4200.5 MHz downlink.

The satellite is constructed in modular form to permit independent assembly, integration, and test of major subsystems. The three modules (Fig. 2) are: communications, support systems, and antenna modules. The primary structural component of the support systems module (SSM) is the thrust tube. The tube forms the spacecraft-to-launch vehicle interface, the antenna module interface, the apogee kick motor interface, and reacts all launch and on-orbit loads.

Development

The first two blocks of spacecraft (FM 1-9) employ an aluminum shell/stringer stiffened thrust tube (Fig. 3). The use of classical airframe technology and materials was dictated by program schedule constraints. During development of the program, R&D efforts were addressed to identify potential mass reductions in the existing spacecraft design to accommodate increases in the payload capacity and extend the life of the satellite. A thrust tube using advanced materials technology was one of the most significant improvements assessed. Material tradeoffs conducted at program start quickly identified graphite fiber-reinforced plastics (GFRP) as the most attractive. Beryllium was evaluated but rejected for a number of reasons, not the least of which being the absence of adequate manufacturers in Europe. Table 1 summarizes the design rationale used to evaluate the different GFRP design concepts.

Two concepts for honeycomb shell construction were evaluated. One solution employed a sandwich with symmetric faceskins; the second, a nonsymmetric faceskin honeycomb sandwich, was chosen for weight considerations. The development design was an aluminum honeycomb sandwich with a thick outer skin stabilized by a thin inner skin. The launch vehicle interface (Marman) ring and the apogee motor interface ring were kept aluminum due to the complexity of manufacturing in graphite, while all other rings plus the four longerons (forming the antenna module interface) were designed in GFRP.

Four main types of verification testing were conducted: load tests on full-scale samples, assembly tests, friction testing on the Marman ring material, and thermal tests. Table 2 summarizes the load testing. These tests resulted in the optimization of the shell/ring interfaces, optimization of the longeron shape and layup, and the sizing of bonded joints. Friction testing of the Marman ring was necessitated by a material change from 5056 to 2618 aluminum. Results indicated identical friction results for both. Thermal testing was made on the apogee motor ring thrust tube interface. High local loads are induced by apogee motor soak-back coupled

Presented as Paper 82-0677 at the AIAA/ASME/ASCE/AHS 23rd Structures, Structural Dynamics and Materials Conference, New Orleans, La., May 10-12, 1982; submitted May 24, 1982; revision received July 18, 1983.

*INTELSAT VA Program Engineering Manager, Western Development Laboratories. Member AIAA.

†Program Manager, INTELSAT Programs, Division Systems Balistiques et Spatiale.

‡Manager of Design, Division Systems Balistiques et Spatiale.

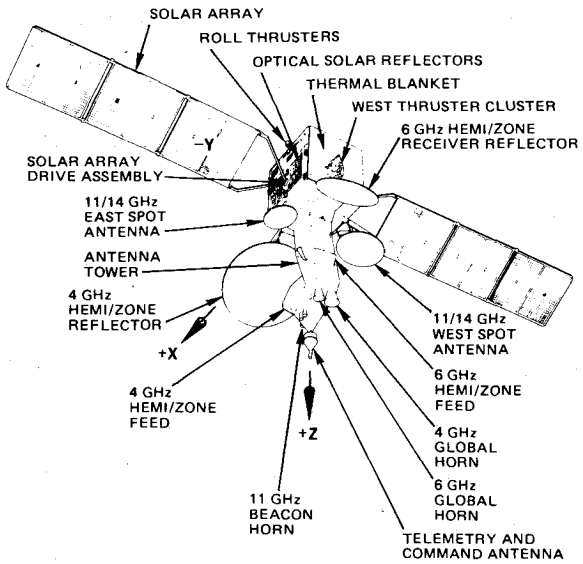

Fig. 1 Spacecraft configuration.

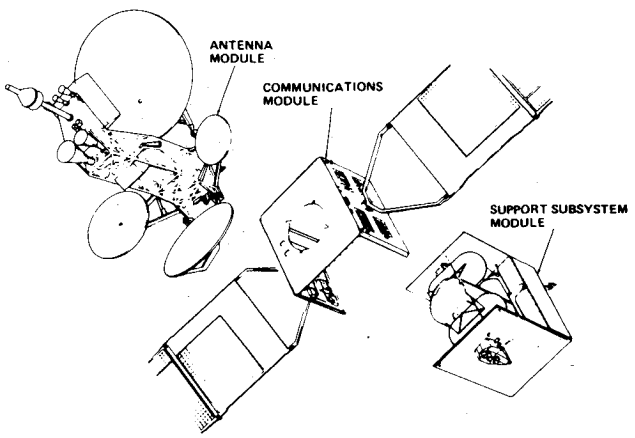

Fig. 2 Spacecraft modular construction.

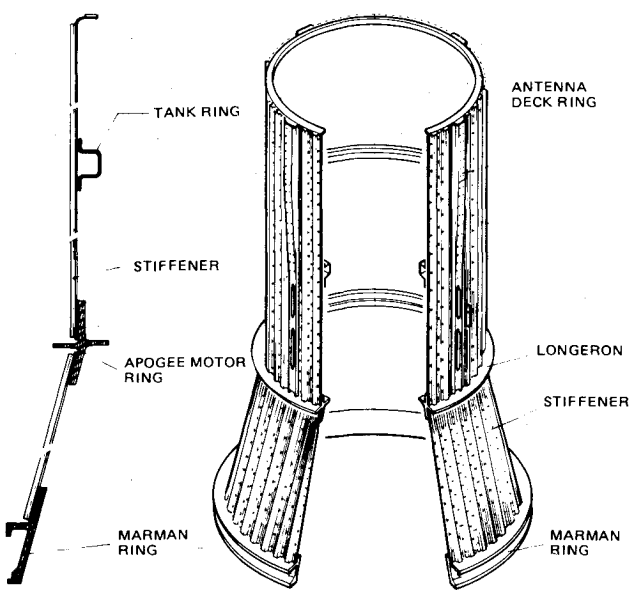

Fig. 3 Aluminum thrust tube.

with the thermal expansion differences between the aluminum ring and GFRP shells. The following design changes were made as a result of the testing plus computer analysis: the addition of rivets to transmit loads during dilation and a modification to the ring cross section increasing its flexibility.

Design Description

The central tube (Fig. 4) is composed of cylindrical and conical shells; the apogee motor (ACS), Marman and antenna deck rings; and the longerons, which form the main body to antenna module interface. The shells are unsymmetric honeycomb panels employing graphite-epoxy faceskins and aluminum honeycomb core. The graphite skins are hybrid mixtures of T300 fabric and unidirectional high-modulus tape. The skins have been optimally sized and ply angles tailored to meet the specific strength/stiffness requirements of each section. The external skins have been sized to carry the

Table 1 Design concept rationale

Design concept	Mass savings	Tooling complexity	Cost	Total
Skin and secondarily bonded stiffeners	3[a]	2	2	7
Skin and integral stiffeners	3	1	1	5
Monocoque	2	4	4	10
Honeycomb shells	4	4	4	12

[a] 1 – Worst condition.

Table 2 Development test summary

Test specimen	Size	Margin of safety[a]
Compression on cylindrical shell	450 × 120 mm	
Without cut out		1.45
With cut out		1.30
Compression on longeron interface	—	0.45
Shear on longeron interface	—	0.53
Antenna deck ring flexure test	—	0.77
Bending on tank ring interface	—	0.39

[a] $(F_{\text{allowable}}/F_{\text{actual}}) - 1$.

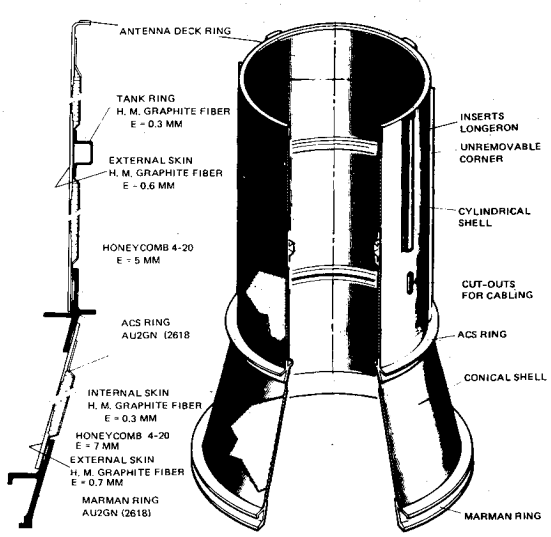

Fig. 4 GFRP thrust tube.

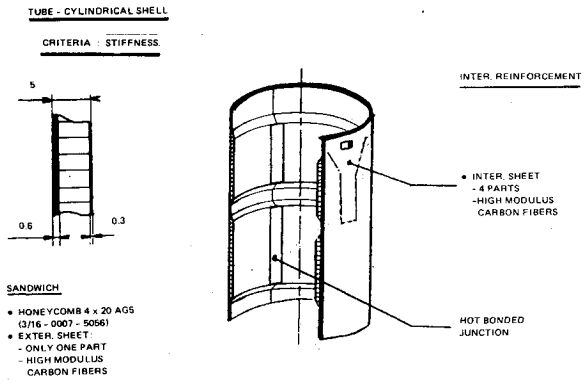

Fig. 5 Cylindrical shell/ring interface.

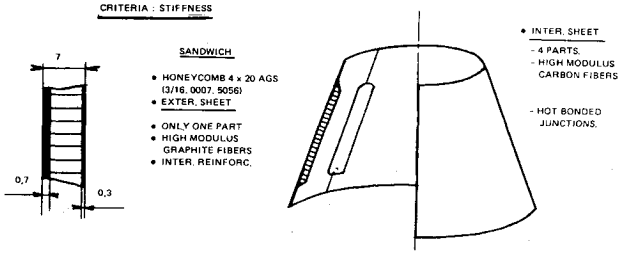

Fig. 6 Conical shell/ring interface.

loads (0.6-mm-thick cylinder skin, 0.7-mm-thick conical skin) with localized doublers (reinforcements) added at attachment points and around cutouts.

A 0.3-mm-thick inner skin, whose function is to stabilize the sandwich, is bonded to 5 mm honeycomb (AG5, 4×20) in the cylindrical section and 7 mm honeycomb (AG5, 4×20) in the conical section. Faceskin to core bonding and skin splicing are achieved with BSL 312L adhesive.

The antenna deck ring is high-modulus graphite-epoxy and is an integral portion of the external cylindrical skin. The tank ring is high-modulus graphite-epoxy, omega-shaped, split and spliced at assembly to ensure that adequate pressure is maintained during the bonding operation. The antenna tower interface fittings are AU2GN bonded into high-modulus graphite-epoxy longerons, which are secondarily bonded and riveted to the external cylinder skin.

Attachments of the communications module webs are accomplished with two aluminum angles—one angle bonded to the cylinder external skin, and the other bolted through integrally bonded inserts in the cylinder sandwich shell. Both the ACS and Marman rings are AU2GN chromic acid anodized in bonding areas and protected by Alodine 1200 in the nonbond areas of the ACS ring only. Both the cylindrical and conical shells are bonded to the ACS and Marman rings with EA9309 adhesive and subsequently riveted. Both shells have "panned edges" (Figs. 5 and 6) at the ring interfaces to ensure load transfer into both faceskins.

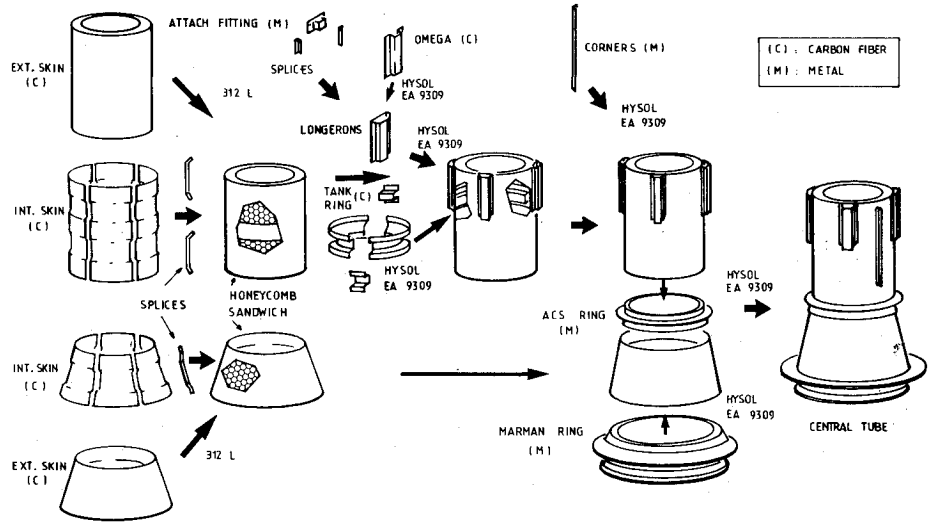

Fig. 7 Central tube assembly sequence.

Table 3 Preliminary ultimate quasistatic launch accelerations, *g*

Main body location	Critical A/C cases				Critical Ariane cases							
	BECO		MECO		1st STG C-O		2nd STG C-O		Max $\propto q$		Apogee motor burn	
	Long	Lat	Long	Lat	Long	Lat	Long	Lat	Long	Lat	Long	Lat
Tower-main body I/F	−9.0	±3.8	+2.3 −6.6	±1.0	+1.1 −7.8	±0.8	−8.6	±0.4	−4.0	±2.8	−7.0	0
Propellant tanks	−9.0	±3.1	+9.3 −9.7	±2.8	+5.8 −8.6	±1.4	−9.0	±0.6	−4.0	±2.2	−7.0	0
Main body	−9.0	±2.2	+2.3 −6.8	±0.6	+1.2 −7.8	±0.3	−8.6	±0.2	−4.0	±1.6	−7.0	0
Case of S/C	−9.0	±1.5	+1.5 −6.6	±0.5	+0.6 −7.7	0	−8.6	0	−4.0	±0.9	−7.0	0

Table 4 Preliminary ultimate internal load

Main body location	Critical A/C loads cases BECO	MECO	Critical Ariane load cases 1st STG C-O	2nd STG C-O	Max $\propto q$
Tower-main body I/F					
Axial, N	−12,880	+4,710	+2,300	−13,060	−6,100
		−9,460	−11,900		
Shear, N	10,830	−2,010	1,200	530	3,240
Moment, N-M	28,080	5,790	2,300	1,150	7,180
Cylinder-cone I/F					
Axial, N	−178,260	+59,500	38,090	−172,250	−78,960
		−130,940	−156,190		
Shear, N	45,123	7,840	3,200	3,200	18,480
Moment, N-M	45,260	8,710	2,180	1,950	18,050
Cone-adapter I/F					
Axial, N		59,500	38,170	−173,040	−79,330
	−179,050	−131,520	−156,900		
Shear, N	46,430	8,150	4,890	3,370	19,250
Moment, N-M	66,670	8,640	4,290	2,440	30,220
Base of S/C					
Axial, N		+59,660	+38,410		
	−181,580	−133,380	−159,180	−175,540	−80,530
Shear, N	46,650	8,110	4,890	3,370	19,530
Moment, N-M	73,560	9,060	5,680	2,810	33,320

I/F = interface; N = Newton; N-M = Newton-meter; S/C = spacecraft

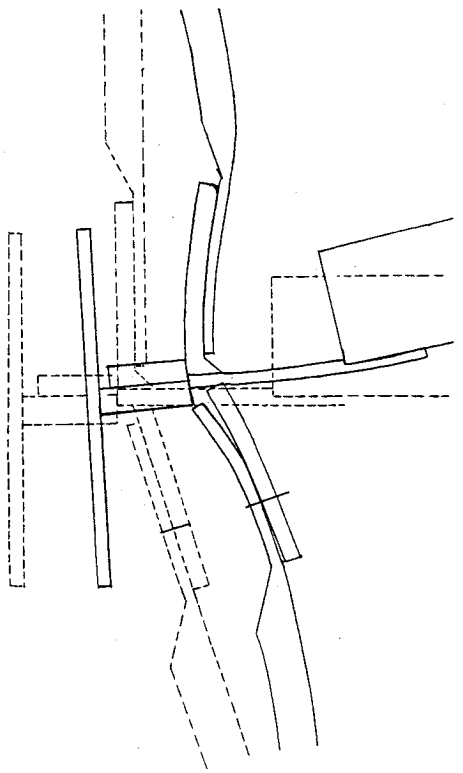

Fig. 8 Apogee motor ring dilation caused by apogee motor soakback.

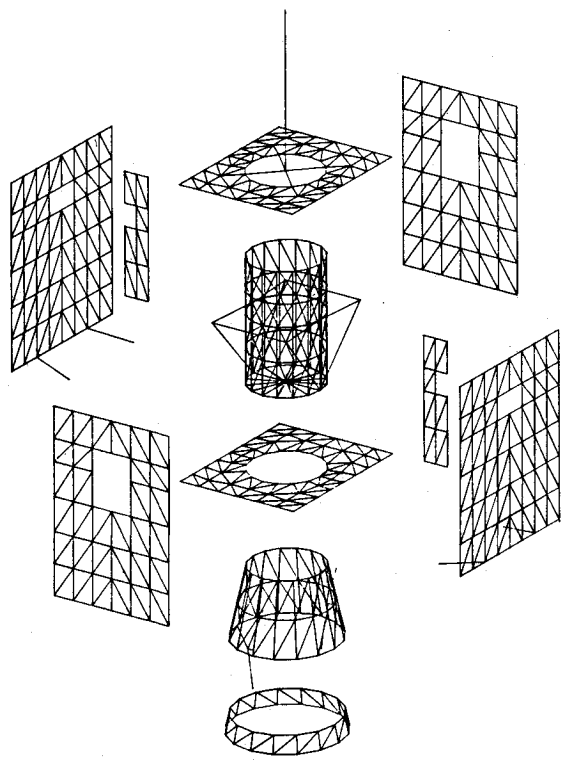

Fig. 9 Thrust tube finite element model.

Assembly

The thrust tube assembly is schematically depicted in Fig. 7. The conical and cylindrical shells are bonded on the apogee motor and Marman rings using the existing central tube assembly tooling. The rings are bonded at room temperature using epoxy adhesive (Hysol EA9309). Following cure, the rivets are added. The final operation involves machining the metallic rings plus the antenna ring to the required geometry.

Analysis

The central tube has been structurally sized by the quasistatic launch vehicle accelerations and stiffness criteria resulting from spacecraft lateral frequency requirements imposed by the launch vehicle contractors. These criteria are listed in Tables 3 and 4. The graphite-epoxy central tube is sized to launch an INTELSAT VA spacecraft on either Atlas-Centaur, Ariane, or the Space Transportation System (STS) launch vehicle.

Maximum line loads were calculated with a BOSOR 4 (Ref. 3) computer program assuming maximum longitudinal and bending moments act simultaneously (these loads actually occur during different mission phases). Structural sizing of the individual members (i.e., faceskin thickness, ply orientations, and sandwich thickness, etc.) was completed using basic material (ply) properties and verified with component

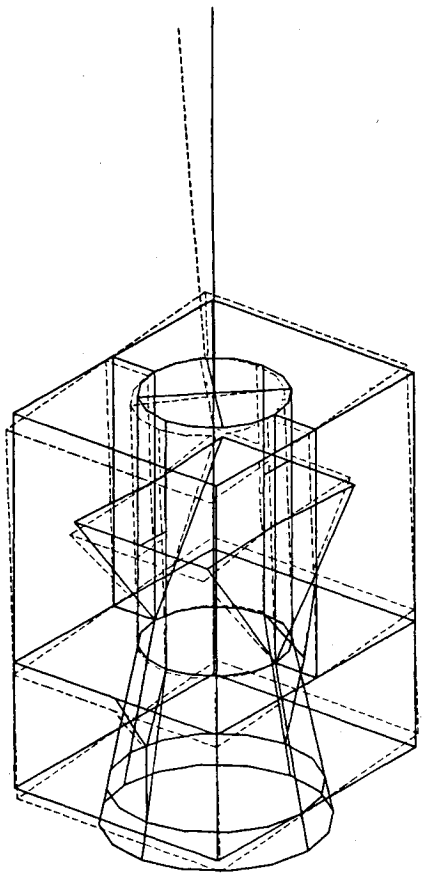

Fig. 10 Spacecraft first mode.

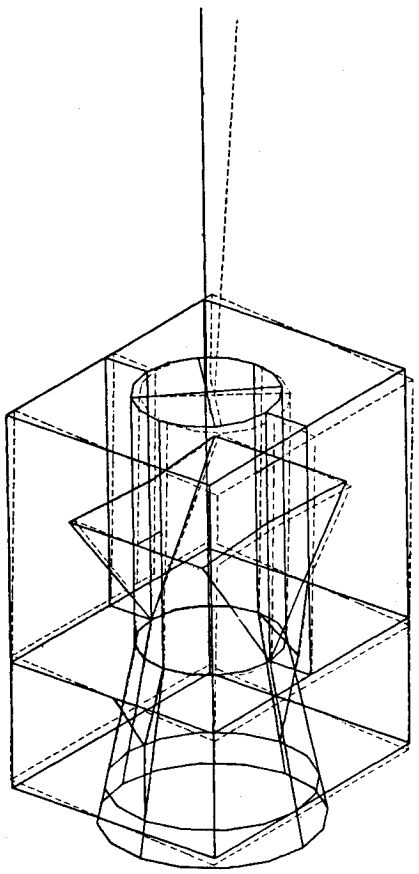

Fig. 11 Spacecraft second mode.

Table 5 Comparison of ELSA and INTELSAT V (basic) static load tests, displacement at ultimate load

	Test $F_y + F_z$			Test $F_x + F_z$		
	ELSA[a]	IT5[b]	IT5/ELSA	ELSA[a]	IT5[b]	IT5/ELSA
Lateral displacement antenna deck	4.15 mm	5.03 mm	1.21	4.80	5.50	1.15
Lateral displacement ACS deck	1.32 mm	1.64 mm	1.24	—	—	—
Rotation at top of central tube	17.5×10^{-4} rad	20.5×10^{-4} rad	1.17	$21.8.10^{-4}$ rad	26.0×10^{-4} rad	1.20

[a]ELSA = GFRP central thrust tube. [b]IT5 = INTELSAT V aluminum tube.

Table 6 Frequency comparison, Hz

Modeshape description	PEM	GEM
Satellite lateral X direction	12	12.5
Satellite lateral Y direction	12	12.5
Satellite 2nd lateral X direction	23	22.5
Satellite 2nd lateral Y direction	26	28
Propellant tanks, longitudinal	27	26
Main body, longitudinal	42	44
Apogee motor, longitudinal	60	60

testing. Special analytic and test emphasis was placed on the shell to metallic ring interface joints.

ACS ring dilation, caused by the apogee motor thermal soak-back, induces severe bending stresses in the panned edge areas of the cylindrical and conical shells (Fig. 8). Extensive component testing has been performed to develop material properties over the expected soak-back temperature extremes. In order to reduce the induced stresses, the cross section of the apogee motor ring has been modified to decrease flange stiffness, and the thermal insulating gasket between the apogee motor mating flange and the ring has been redesigned to reduce conductive coupling.

Finite element stiffness and mass models were prepared and used for frequency and mode shape calculations. Stiffness characteristics of the thrust tube were represented by the finite element computer model shown in Fig. 9. Mass characteristics of the spacecraft were modeled by judiciously lumping the equipment at the appropriate station. Figures 10 and 11 represent the first two modes of the spacecraft.

A prototype tube has been manufactured and subjected to both ultimate static loads and acceptance level dynamic testing. Figure 12 schematically depicts the static load test arrangement. The type and magnitude of the applied loads were identical with those used during qualification testing of the aluminum tube, and simulate line loads induced during various launch and preoperational phases. Strain gage results show a good linearity of the strain/load curves up to ultimate load with no significant residual strains present after unloading. A comparison of the test results for the GFRP tube and the aluminum qualification tube is presented in Table 5.

This displacement data indicated that the graphite tube is laterally stiffer than the aluminum tube. To assess the impact

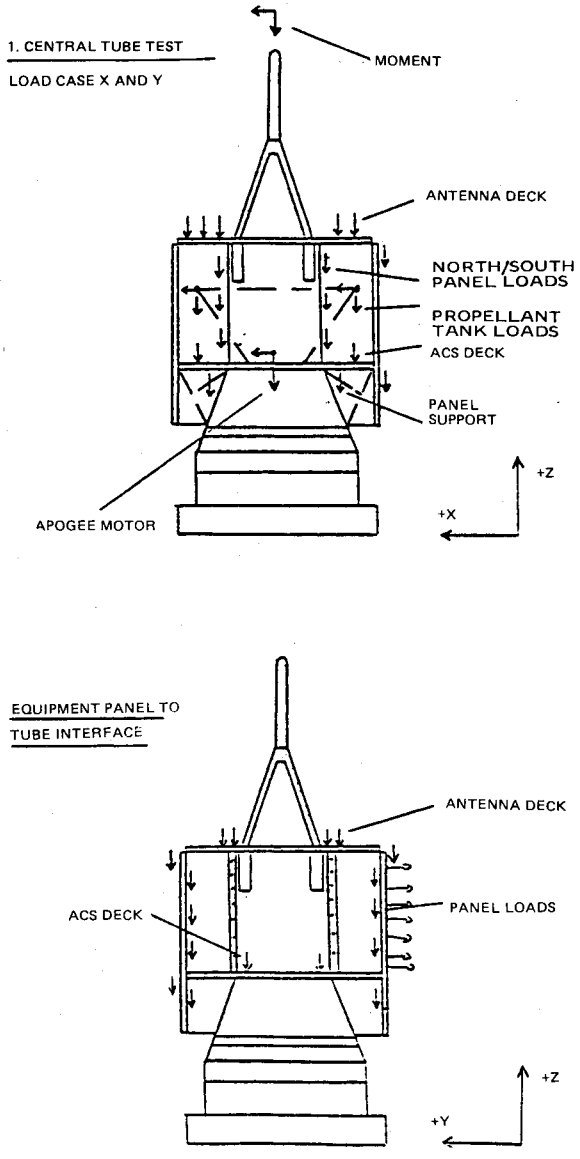

Fig. 12 Static load test schematic of applied loads.

of the stiffer tube on basic spacecraft frequencies, the prototype tube was integrated into the INTELSAT V Proto Engineering Model (PEM) spacecraft and subjected to spacecraft acceptance level sine vibration testing. The PEM is an exact duplicate of the working spacecraft, except that it utilizes mass dummies for various box components. Test results indicate no significant frequency differences between the PEM (Proto Engineering Model plus aluminum thrust tube) and the GEM (Proto Engineering Model plus GFRP thrust tube) configurations. Results are summarized in Table 6. A slight shift in first-mode frequencies of some components was noted, but overall spacecraft frequencies remained essentially unchanged.

Summary

The design of a sophisticated, lightweight, high-performance structure for use in space has been described. Weight savings requirements in excess of 9 kg were satisfied by use of graphite-epoxy material. Features of the structure design include:

1) Simple honeycomb sandwich shell configuration for efficient use of unidirectional graphite material.

2) Computer optimized ply orientations for low structural weight.

3) Bonded joints with room-temperature cure adhesives for light weight and ease of assembly.

4) Structurally qualified for launch on either the Atlas-Centaur, Ariane, or Space Transportation System.

5) Full interchangeability with the existing aluminum tube.

Acknowledgment

The work described herein was sponsored in part by the International Telecommunications Satellite Organization (INTELSAT). Any views expressed herein are not necessarily those of INTELSAT.

References

[1] Rusch, R.J., Johnson, J.J., and Baer, W., "Intelsat V Spacecraft Design Summary," *1978 Communications Satellite Systems Conference*, San Diego, Calif., 1978, pp.

[2] Barberis, N.J. and Hoeber, C.F., "Design Summary of the Intelsat VA Spacecraft," *1982 Communications Satellite Systems Conference*, San Diego, Calif., 1982, pp.

[3] "Stress, Stability and Vibration of Complex Branched Shells of Revolution, Analysis and Users Manual," LMSC-D-243605, 1972.